968 © *1980 The Chemical Society of Japan* *Bull. Chem. Soc. Jpn.*, *53*, *968—974 (1980)* [Vol. 53, No. 4

An Application of the Extended Principal Component Analysis to Circular Dichroism and Optical Rotatory Dispersion. A Case of Poly(α-L-glutamic acid) in the Helix-Coil Transition Region

Kiwamu YAMAOKA,* Takumi MATSUDA, and Mineo TAKATSUKI
Faculty of Science, Hiroshima University, Higashisenda-machi, Hiroshima 730

(Received June 4, 1979)

The extended principal-component-analysis (PCA) method has been applied to circular dichroism (CD) and optical rotatory dispersion (ORD). The validity of this method has been examined with ideal binary and ternary equilibrium systems, for which the data CD spectra and ORD curves were computer-generated. Satisfactory results were obtained for these multicomponent optically active systems. As an example, the ultraviolet CD spectra of poly(α-L-glutamic acid) in the pH-induced helix-coil transition region were analyzed with the PCA procedure. By the extended PCA method, the pure CD spectra for both helix and random-coil conformations and the helix fractions in the transition region were determined from eight experimentally obtained CD spectra. By introducing an empirical parameter α into the Henderson-Hasselbalch equation, the helix-coil transition curve was reproduced reasonably well.

Many vectorial methods have been developed for the analysis of the optical spectra which result from either the light-absorbing species in chemical equilibria or the components in conformational equilibria.[1-18)] The total number of species or conformers (both simply denoted as components) in such equilibria can be determined by means of rank analysis,[1-5)] factor analysis,[6)] and principal component analysis.[7-13)] The principal component analysis (hereafter abbreviated as the PCA method) was extended by Kankare[10)] and by the present authors[11-13)] in order to resolve the observed optical spectra into the spectra of individual components involved in an equilibrium system.

The concentrations of individual components may be determined by factor analysis,[6)] the least-square-curve-fitting method,[14-17)] and the reciprocal function method.[18)] Some of these methods have been applied to the circular dichroism (CD) spectra and optical rotatory dispersion (ORD) curves of optically active biopolymers in solution in order to interpret the observed optical data in terms of the various conformations.[5,6,14-18)] In these methods, however, an appropriate reference spectrum must be assumed for each component. It is highly desirable to obtain the number of unknown polymer conformations (*i.e.*, components), the pure CD spectra or ORD curves of these components, and the fraction of each component, without assuming any reference spectra *a priori*. Therefore, the application of the PCA method to both CD and ORD is attempted in this work.

The extended PCA method has been utilized to analyze the absorption spectra of associative dyes in the monomer-dimer and acid-base equilibria[11)] and in the binding with polyelectrolytes.[12,13)] Two obvious physical conditions can be attached to the analysis of a given system: the absorbance and the concentration of each component are always non-negative. However, the CD and ORD are both signed quantities. The only remaining physical restriction is the non-negative concentration. Nevertheless, the extended PCA method is applicable to the CD and ORD data in a manner similar to the absorption, yielding the proper equilibrium scheme, the equilibrium constant, the number of optically active components, and the component CD spectra or ORD curves. As an illustration, the pH-induced change of the CD spectra of poly(α-L-glutamic acid) will be dealt with.

The Outline of the Extended PCA Method

Since the extended PCA method has previously been described in detail,[11,12)] the procedure pertaining to the CD and ORD data will be given here. Suppose that m data CD spectra or ORD curves are experimentally available for a chemical system in equilibrium, which contains p optically active components, and that each data spectrum is a sum total of the p component spectra. The purpose of the extended PCA method is to determine the unknown number of components, p, and then the concentration and the pure spectrum of each component.

Over a certain wavelength region, m data CD spectra or ORD curves may be measured for m solutions, each of which contains a maximum of p components in equilibrium. If the Lambert-Beer-type additivity holds for the component CD spectra or ORD curves, as in the case of absorption spectra, the data matrix, $\boldsymbol{D}_\theta$ or $\boldsymbol{D}_\phi$, may be expressed as the product of the concentration matrix, $\boldsymbol{C}$, and the CD or ORD spectral matrix, $\boldsymbol{\theta}$ or $\boldsymbol{\phi}$, of the p components measured at n selected wavelengths:

$$\boldsymbol{D}_\theta = \boldsymbol{C\theta} = \begin{bmatrix} C_{11} & \cdots & C_{1p} \\ \vdots & C_{ij} & \vdots \\ C_{m1} & \cdots & C_{mp} \end{bmatrix} \begin{bmatrix} \theta_{11} & \cdots & \theta_{1n} \\ \vdots & \theta_{jk} & \vdots \\ \theta_{p1} & \cdots & \theta_{pn} \end{bmatrix}, \tag{1}$$

or:

$$\boldsymbol{D}_\phi = \boldsymbol{C\phi} = \begin{bmatrix} C_{11} & \cdots & C_{1p} \\ \vdots & C_{ij} & \vdots \\ C_{m1} & \cdots & C_{mp} \end{bmatrix} \begin{bmatrix} \phi_{11} & \cdots & \phi_{1n} \\ \vdots & \phi_{jk} & \vdots \\ \phi_{p1} & \cdots & \phi_{pn} \end{bmatrix}. \tag{2}$$

In these expressions, C_{ij} denotes the concentration of the jth component in the ith data spectrum, while

θ_{jk} and ϕ_{jk} are the θ and ϕ quantities of the jth component at the kth selected wavelength λ_k respectively.

A second-moment matrix, $\boldsymbol{A}$, is constructed from the data matrix as:

$$\boldsymbol{A} = {}^t\boldsymbol{D}_\theta \boldsymbol{D}_\theta \text{ or } \boldsymbol{A} = {}^t\boldsymbol{D}_\phi \boldsymbol{D}_\phi. \quad (3)$$

The eigenvalues $\Lambda_i(i=1,\ n)$ and the corresponding eigenvectors, $\boldsymbol{e}_i$, can be calculated from the $\boldsymbol{A}$ matrix by diagonalization. The relative magnitude of Λ_i permits us to determine the number of significant components.[11,12)] Two new matrices, $\boldsymbol{f}$ and $\boldsymbol{t}$, are introduced as follows:

$$\boldsymbol{D}_\theta = \boldsymbol{f}_\theta \boldsymbol{e}_\theta \text{ or } \boldsymbol{D}_\phi = \boldsymbol{f}_\phi \boldsymbol{e}_\phi, \quad (4)$$

and:

$$\boldsymbol{\theta} = \boldsymbol{t}_\theta \boldsymbol{e}_\theta \text{ or } \boldsymbol{\phi} = \boldsymbol{t}_\phi \boldsymbol{e}_\phi. \quad (5)$$

The $\boldsymbol{e}$ matrix, consisting of p eigenvectors, is transformed to the $\boldsymbol{D}$ matrix by the $\boldsymbol{f}$ matrix, and also to the $\boldsymbol{\theta}$ and $\boldsymbol{\phi}$ matrices by the $\boldsymbol{t}$ matrix. The concentration matrix, $\boldsymbol{C}$, is given as:

$$\boldsymbol{C} = \boldsymbol{f}\boldsymbol{t}^{-1}. \quad (6)$$

Equations 4—6 indicate that the pure spectra of unknown components and their concentrations contributing to each data spectrum may be evaluated, once the elements of the $\boldsymbol{t}$ matrix are available.

In order to determine the $\boldsymbol{t}$ matrix, an appropriate equilibrium scheme must be selected.[11-13)] The general expression for the scheme may be written as:

$$K = \prod_{i=1}^{q} [X_i]^{\nu i}, \quad (7)$$

where K is the equilibrium constant, X_i is the ith component, which may be either optically active or inactive, and the ν is the stoichiometric coefficient. The brackets denote the molar concentration. It should be noted that the number of q is always larger than, or equal to, p. The coefficient of variation, S, is defined as:

$$S = \left[\frac{1}{m}\sum_{j=1}^{m}(K_j - \bar{K})^2\right]^{1/2} \Big/ \bar{K}, \quad (8)$$

where $\bar{K}$ is the mean equilibrium constant averaged over m equilibrium constants $K_j(j=1,\ m)$, by which an equilibrium (Eq. 7) is specified in m solutions (*i.e.*, m data spectra). Hence, the magnitude of the S value is the criterion for selecting the proper scheme for a given multicomponent equilibrium system.[11,12)] It should be noted that, in any equilibrium system in which both L- and D-isomers of an optically active compound are involved, the $\boldsymbol{C}$ matrix (Eq. 6) describes only the difference in concentration between the two isomers. Thus, the number of components will be one instead of two in a racemization reaction (*e.g.*, L-isomer$\rightleftarrows$D-isomer).

Results and Discussion

Ideal Binary System. Consider the following chemical equilibrium, in which an optically active chemical species, X_2, dissociates into an optically active species, X_1^-, and a proton:

$$X_2 \rightleftarrows X_1^- + H^+. \quad (9)$$

The quilibrium constant, K_a, is given by:

$$K_a = \frac{[X_1^-][H^+]}{[X_2]}. \quad (10)$$

When $K_a = 1 \times 10^{-6}$ M ($=$mol/dm^3) and when the pH of the system is varied from 7 to 5 by 0.25 pH units, a set of nine data CD spectra or ORD curves will be computer-generated, according to Eq. 10, by a linear combination of the hypothetical, component spectra of the X_1^- and X_2 species.

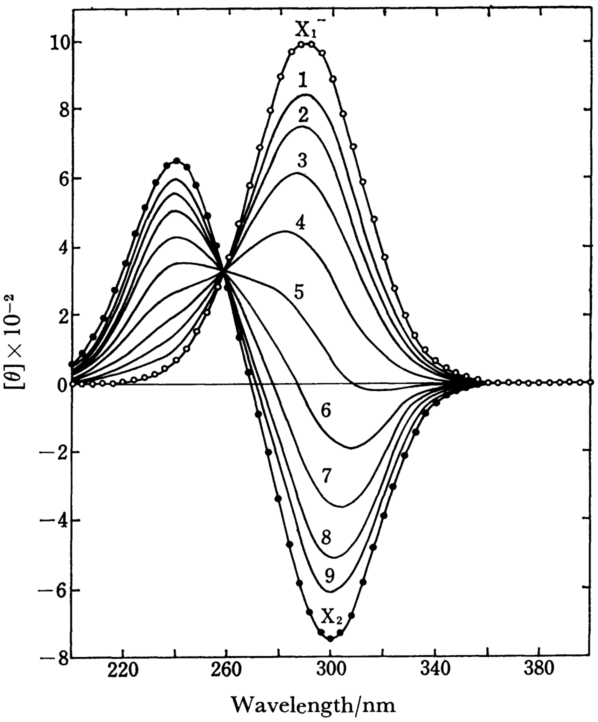

Fig. 1. The hypothetical component CD spectra (X_1^-, X_2) and the generated data CD spectra (1—9) for an ideal binary equilibrium system. The data spectra were computed according to Eq. 10 and expressed with the molar ellipticity $[\theta]$. Symbols (○ and ●) indicate the estimated pure component spectra. The pH values of spectra 1 and 9 were set to be 5 and 7, respectively. For other details, see text.

The Case of CD. Figure 1 shows the component CD spectra of X_1^- and X_2. They were synthesized from a single Gaussian curve and a more complex Gaussian curve respectively. By using these component spectra, nine data CD spectra (Nos. 1—9) were computed at 4 nm intervals between 200 and 400 nm and at nine pH values. It is interesting to note that the data CD spectra (Nos. 1—9) all cross each other at a single wavelength near 260 nm, which may be termed the *isoelliptic* or *isodichroic* point by analogy with the isosbestic point of the absorption spectra. The presence of this point for a set of experimentally observed spectra should be taken as evidence for the two-optically-active-component system.

The supposedly unknown number of components in the equilibrium scheme (Eq. 9) is found from the eigenvalues of the second-moment matrix constructed from the nine data spectra. Figure 2(a) shows that a large gap exists between the second and third components. The gap

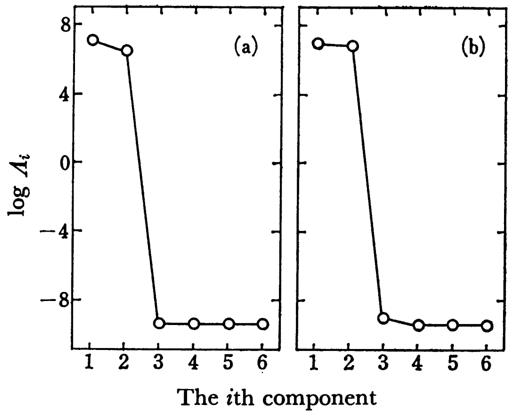

Fig. 2. The relation between eigenvalue Λ_i and the *i*th component for the ideal binary system. (a) the data CD spectra in Fig. 1 and (b) the data ORD curves in Fig. 3.

indicates the correctness of the computing procedure for the assumed binary system. Analysis of the data spectra with Eq. 10 produced the values of 1×10^{-5} for S and 1×10^{-6} M for $\bar{K}_a$, the latter agreeing excellently with the preset value. The pure CD spectra of the X_1^- and X_2 components (open and filled circles) were reproduced quite well, as is shown in Fig. 1. The relative error between the computer-generated input data spectra and the iterated output component spectra was always less than 0.01% throughout the present work.

In actual CD measurements, experimental difficulties, such as the high absorbance and low CD signal of a solution, often limit the measurable wavelength region. Therefore, the 200—400 nm region was reduced to two narrower wavelength regions of 280—400 nm and 320—400 nm in this simulation, and the same PCA procedure as above was applied to each region. The values of $\bar{K}_a$ and S were all the same regardless of the wavelength region. This is conceivable because no experimental error was taken into account in the ideal system. Conversely, however, it is not necessary to cover the entire wavelength region where the complete CD features prevail if CD measurements are carried out with a sufficiently high accuracy.[11]

In order to examine whether or not the given equilibrium scheme (Eq. 9) has been determined uniquely, a check is made with a general equilibrium scheme given as:

$$n\mathrm{X}_2 \rightleftarrows n\mathrm{X}_1^- + m\mathrm{H}^+. \qquad (11)$$

The corresponding equilibrium constant, K_b, is written as:

$$K_b = \left(\frac{[\mathrm{X}_1^-]}{[\mathrm{X}_2]}\right)^{\alpha}[\mathrm{H}^+], \qquad (12)$$

where $\alpha = n/m$. The data spectra in Fig. 1 were analyzed with the aid of the various values of α in Eq. 12 in order to compare the variation in S with the exponent α. The results are given in Table 1, which shows that the value of S increases as the α value deviates from unity. This trend is what should be expected for the present binary system, since the equilibrium scheme was generated with $\alpha = 1$.

TABLE 1. THE DEPENDENCE OF THE S VALUES ON THE PARAMETER, α, IN EQUILIBRIUM EXPRESSIONS (Eqs. 12 AND 16) FOR THE IDEAL BINARY AND TERNARY SYSTEMS

α	Binary System (CD and ORD in 200—400 nm)[a]	Ternary System (CD and ORD in 200—400 nm)[a]
0.7	0.144	0.0012
0.8	0.082	0.0009
0.9	0.035	0.0005
1.0	0.000	0.0000
1.1	0.026	0.0009
1.2	0.040	0.0018
1.3	0.062	—
1.4	0.074	—

a) Identical results were obtained for both CD and ORD in the two narrower wavelength regions of 280—400 nm and 340—400 nm respectively.

The Case of ORD. Experimental difficulties often forbid the CD spectra to be measured in the wavelength region where positive or negative bands are anticipated. In this case, the application of the PCA method is impracticable. The ORD is a dispersive quantity and displays the Cotton effect associated with a CD band. The peak or the trough of the Cotton effect, together with the sign and magnitude, can often be observed on the long-wavelength side removed from the CD band. In ORD measurements the optical path length of a sample solution may easily be increased outside the absorption peak. These facts lead to the usefulness of the highly accurate data ORD curves for the rigorous PCA treatment. The ORD data are thus valuable in complementing the shortcomings of the corresponding CD data. Therefore, the PCA procedure

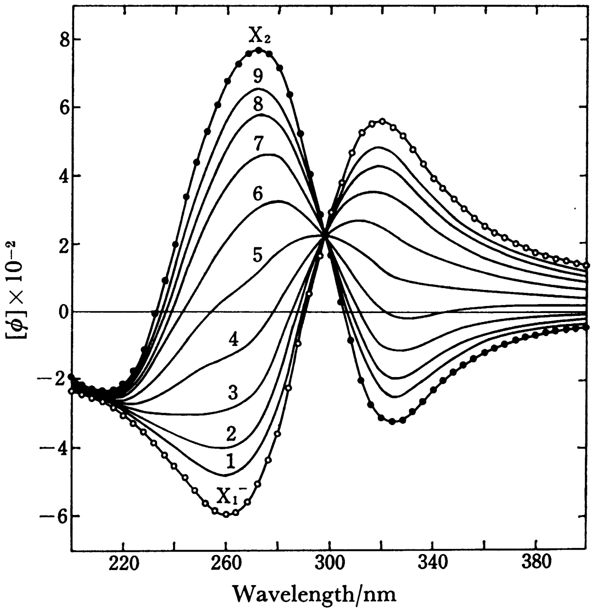

Fig. 3. The hypothetical component ORD curves (X_1^-, X_2) and the generated data ORD curves (1—9) expressed with the molar rotation $[\phi]$ for the same binary system as in Fig. 1. Symbols (○ and ●) indicate the estimated pure component curves.

is applied to the ORD data of the same ideal binary system as above.

Consider the same equilibrium scheme (Eq. 9) and the expression Eq. 10 with $K_a=1\times10^{-6}$ M. The hypothetical ORD curves for the X_1^- and X_2 components were computed from the corresponding CD spectra by the use of the Kronig-Kramers transform:[19,20]

$$[\phi(\lambda)] = \frac{2}{\pi}\int_{\lambda'_1}^{\lambda'_n}[\theta(\lambda')]\frac{\lambda'}{\lambda^2-\lambda'^2}\mathrm{d}\lambda', \qquad (13)$$

where $[\theta]$ and $[\phi]$ are the molar ellipticity and the molar rotation respectively. The nine data ORD curves were similarly computed from the corresponding data CD spectra and are shown in Fig. 3. The *unknown* number of optically active components present in the equilibrium was determined from the eigenvalues using these curves. The result is shown in Fig. 2(b), in which a large gap again exists between the second and third components, indicating the system to be in a two-component equilibrium.

The PCA procedure was applied to this binary system using the general equilibrium scheme (Eq. 11). The results are given in Table 1. As in the CD treatment, the best simulation was obtained with $\alpha=1$ in Eq. 12, resulting in $S=1\times10^{-5}$ and $\bar{K}_b=1\times10^{-6}$ M, all of which are very close to the preset values. The pure ORD curves for X_1^- and X_2 (open and filled circles) resulting from the analysis of the nine data curves are in excellent agreement with the component ORD curves (X_1^- and X_2), as is shown in Fig. 3. As in the case of CD, the wavelength range was reduced to two narrower regions of 280—400 nm and 340—400 nm. The narrowing of the selected wavelength region did not affect the results. This indicates that even the *normal* ORD curves removed from the Cotton effect region are useful for extracting information on the equilibrium by the PCA method. Figure 3 suggests that the observed ORD curves should all cross each other at a wavelength which may be termed the *isodispersive point* if the concentration of one of the components is varied relative to the other in a two-component equilibrium system.

Ideal Ternary System. Consider a more complex equilibrium system which is composed of three optically active components, X_1, X_2, and X_3. The following equilibrium scheme is assumed:

$$X_1 + X_2 \rightleftarrows X_3, \qquad (14)$$

and:

$$K_c = \frac{[X_3]}{[X_1][X_2]} \qquad (15)$$

The CD spectrum and the corresponding ORD curve for each component were constructed in the same manner as in the binary system; they are shown in Figs. 4(a) and (b) respectively. Thirteen data CD spectra were generated (Nos. 1—13) from three pure component CD spectra with $K_c=5\times10^5$ M^{-1} in Eq. 15. In this case, the X_1 component was assumed to be titrated with X_2 to yield X_3 in such a way that the ratio of the concentration of the added X_2 to the initial concentration of X_1 was varied from 0.1 to 1.3. Since this series of data CD or ORD was synthesized from three components, the spectral features are very complicated, varying with the concentrations of the reactants, X_1 and X_2; *viz.*, no isoelliptic or isodispersive point exists.

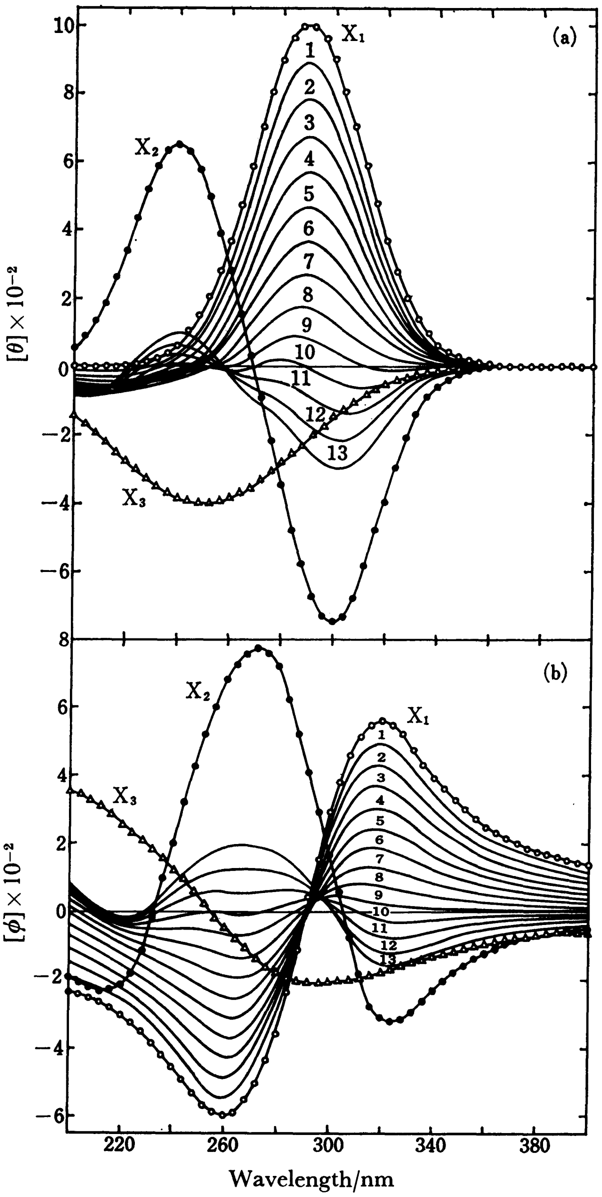

Fig. 4. The hypothetical component CD spectra and ORD curves (X_1, X_2, X_3) and the generated data (1—13) for an ideal ternary equilibrium system: (a) CD data were calculated from Eq. 15. (b) ORD data were computed from the corresponding CD spectra according to Eq. 13. Symbols (○, ●, and △) indicate the estimated pure component CD and ORD.

No visual inspection of these data CD spectra or ORD curves allows us to predict the number of optically active components involved in this equilibrium. The number was determined to be three by the PCA procedure, as is shown in Figs. 5(a) and (b). A large gap of eigenvalues exists between the third and fourth components, confirming the presence of three components. The most suitable expression for the chemical equilibrium has been searched for in the various equilibrium schemes by the use of the following general expression:

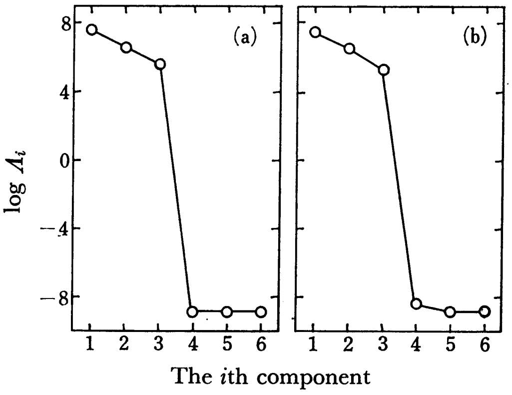

Fig. 5. The relation between eigenvalue A_i and the ith component for the ideal ternary system. (a) the CD data and (b) the ORD data in Fig. 4.

$$K_d = \left(\frac{[X_3]}{[X_1]}\right)^{\alpha}[X_2]^{-1}, \tag{16}$$

in which the parameter, α, was varied from 0.7 to 1.2. The trial-and-error computer analysis produced the minimized S value of 1×10^{-5} at $\alpha=1$ and $\bar{K}_d=5\times10^5$ M^{-1}. These values all satisfy the originally assumed equilibrium conditions. A good agreement is seen between the component CD spectra or ORD curves originally set for the computer-generation and those determined from the thirteen data spectra by the PCA procedure, as is indicated by circles and triangles in Figs. 4(a) and (b). The S value increases as the α is varied from the preset value of unity. Thus, Eq. 15 is discriminated from the remainder as the most appropriate expression. No effect was observed on the final result when the wavelength region covered for the selected wavelengths was restricted, as in the case of the binary system.

A Real System of Poly(α-L-glutamic acid) in the Helix-Coil Transition Region. To the eight data CD spectra shown in Fig. 6, the PCA procedure was applied in order to determine the number of components (or conformations) present in poly(Glu) in the pH range of 5.13—7.49.[21] The eigenvalues are plotted against the components in Fig. 7, in which a considerable gap is observed between the second and third components. Since the difference in logA_i between the first and the third components is about 4, the poly(Glu) system can be concluded to consist of two components. This is the result that has been anticipated from the data CD spectra which all cross each other at 203.5 nm (the isoelliptic point).[21] These components may be assigned to the helical and random-coil conformations of poly(Glu).

Although the mechanism of the pH-induced helix-coil transition has not yet been fully resolved, the pH-induced transition may be formally written as:

$$\text{Helix} \rightleftharpoons \text{Coil} + \text{H}^+ \tag{17}$$

with an equilibrium constant, K. The equilibrium expression for scheme (17) is difficult to derive theoretically. Hence, the modified Henderson-Hasselbalch equation[22,23] is utilized under the assumption that it represents the experimental data by adjusting the parameter, α:

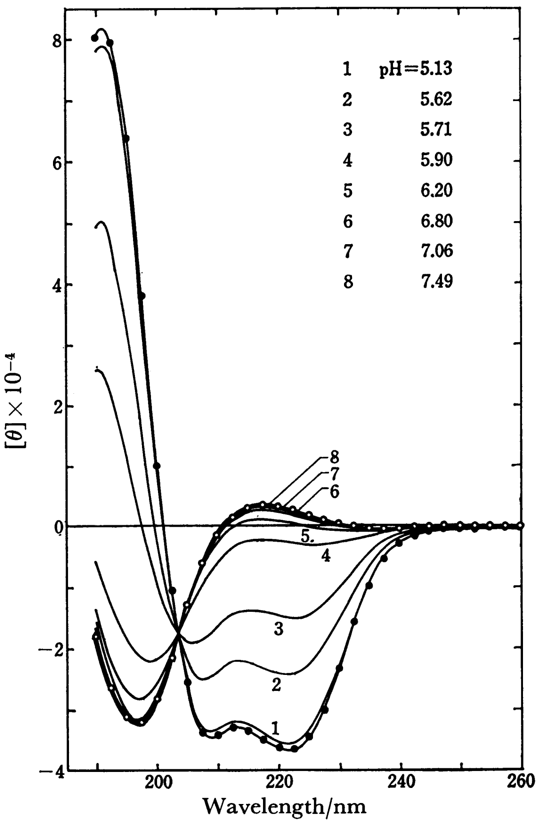

Fig. 6. The observed CD spectra of poly(α-L-glutamic acid) in the helix-coil transition region and the estimated pure helix (—●—) and pure coil (—○—) CD spectra. The data spectra are expressed with the molar ellipticity [θ] and taken from Ref. 21, to which the experimental details should be referred. The residue concentration was 8.0 mM in *ca.* 7.5 mM NaCl solutions throughout the pH range.

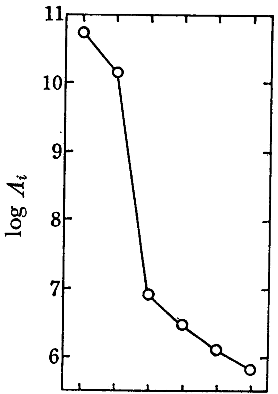

Fig. 7. The relation between the eigenvalue A_i and the ith component for the poly(Glu) system shown in Fig. 6.

$$\text{pH} = \text{p}K - \alpha \log\frac{[\text{Helix}]}{[\text{Coil}]}, \tag{18}$$

where [Helix] and [Coil] denote the concentrations of the helix and coil conformations of poly(Glu). Equation 18 is quite suitable for the computer analysis, because it contains a single adjustable parameter, α, similar to the one that was determined uniquely in the ideal systems.

Table 2. The dependence of the S and p$\bar{K}$ values on the parameter, α, of the modified Henderson-Hasselbalch equation applied to the helix-coil transition of poly(Glu)

α	S	p$\bar{K}$
0.2	0.0262	5.75
0.3	0.0198	5.76
0.4	0.0150	5.74
0.5	0.0125	5.68
0.6	0.0132	5.60
0.7	0.0172	5.52
0.8	0.0229	5.41
0.9	0.0294	5.29
1.0	0.0368	5.18

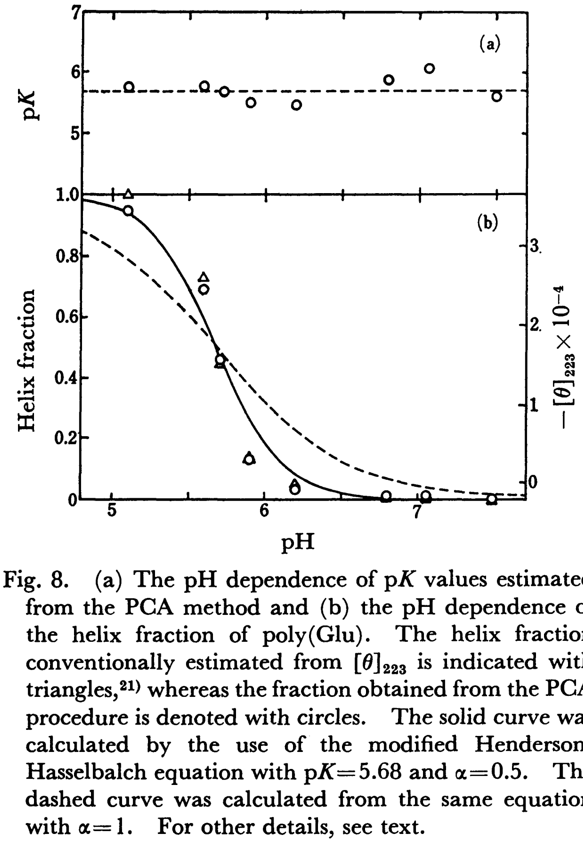

Fig. 8. (a) The pH dependence of pK values estimated from the PCA method and (b) the pH dependence of the helix fraction of poly(Glu). The helix fraction conventionally estimated from $[\theta]_{223}$ is indicated with triangles,[21] whereas the fraction obtained from the PCA procedure is denoted with circles. The solid curve was calculated by the use of the modified Henderson-Hasselbalch equation with p$\bar{K}$=5.68 and α=0.5. The dashed curve was calculated from the same equation with α=1. For other details, see text.

The parameter should be considered to be only an empirical one which implicitly contains the effects on the conformational change of the ionic strength, the electrostatic surface potential, the shape factor, and other polyelectrolyte properties. The results of the PCA procedure are given in Table 2. Since the concentration of protons is measured in terms of pH, the S value is evaluated in terms of pK rather than K; it reaches its minimum at α=0.5. The pK values for eight data CD spectra are plotted against pH in Fig. 8(a), where the average pK value, p$\bar{K}$, is 5.68 (dashed line). The pK values deviate from p$\bar{K}$ in a random fashion over the entire pH range, 5.1—7.5. This indicates that the PCA procedure is correctly applied to the appropriate equilibrium scheme.

The helix fraction at a given pH, which is defined as [Helix]/([Helix]+[Coil]), can be calculated from Eq. 18 with p$\bar{K}$=5.68 and α=0.5. The results are plotted by the solid curve in Fig. 8(b). This curve is in good agreement with the helix fraction calculated from the C matrix by the PCA procedure (circles). Figure 8(b) also indicates that poly(Glu) is in the random-coil form almost completely at pH 7, but that nearly 95% of poly(Glu) is in the helix conformation at pH 5. The helix fraction has usually been calculated from the experimentally obtained molar ellipticity $[\theta]$ at a selected single wavelength, often at 222 or 223 nm, with the empirically chosen values of $[\theta]$ at two reference pH's which are assigned to the complete coil and helix conformations.[16,24] The results obtained from the PCA method make it clear that the conventional method (triangles) also yields a similar helix-coil transition curve.

It is worth emphasis that the modified Henderson-Hasselbalch equation with the single parameter, α, can describe the pH-induced helix-coil transition of poly(Glu) reasonably well over an entire pH range, permitting the evaluation of the helix fraction by the extended PCA method. The unmasked CD spectra for the complete helix and coil conformations are shown by filled and open circles respectively in Fig. 6. While the observed CD spectra at pH>7.1 may be considered as the pure CD spectrum for a coil, the pure CD spectrum for a helix is slightly higher than the highest observed CD spectrum at pH 5.13. Thus, the conventional estimation from $[\theta]_{223}$ would overestimate the helix fraction by approximately 5% in the low-pH region.

Finally, the results of the present work encourage the analysis of more complicated multicomponent systems, such as polylysine in alkaline solutions, in which three conformations (α-helix, β-structure, and random-coil) coexist, or natural proteins which undergo denaturation by environmental changes. For this purpose, our instrumental techniques must be improved so as to give highly accurate data worthy of the elaborate PCA procedure. The extended PCA method has so far been proved applicable to such optical spectra as the absorption, CD, and ORD. It may also be employed to analyze other spectral data like NMR, for which a Lambert-Beer-type linear combination rule holds.

Conclusion

The features of the extended PCA method as applied to both CD and ORD data of multicomponent equilibrium systems are: (1) the number of optically active components may be deduced from a set of data CD spectra or ORD curves (except for enantiomers), and (2) the unknown pure spectra of those components are determined by analyzing the data with appropriately chosen equilibrium expressions. Thus, the extended PCA method requires no presumption of the number of components (or conformations) or their characteristic spectra; these quantities must, by contrast, be assumed in other analytical methods. The application of the extended PCA method to the CD data of poly(Glu) has confirmed that the pH-induced helix-coil transition can be described by a two-state equilibrium model over the pH range of 5.1—7.5.

References

1) R. M. Wallace, *J. Phys. Chem.*, **64**, 899 (1960).

2) R. M. Wallace and S. M. Katz, *J. Phys. Chem.*, **68**, 3890 (1964).

3) S. Ainsworth, *J. Phys. Chem.*, **65**, 1968 (1961).

4) D. Katakis, *Anal. Chem.*, **37**, 876 (1965).

5) C. March, C. Schneider, and L. Brehamet, *Biopolymers*, **17**, 1065 (1978).

6) R. W. Coombs, J. A. Verpoorte, and K. B. Easterbrook, *Biopolymers*, **15**, 2353 (1976).

7) T. W. Anderson, *Ann. Math. Statist.*, **34**, 122 (1963).

8) W. H. Lawton and E. A. Sylvestre, *Technometrics*, **13**, 617 (1971).

9) N. Ohta, *Anal. Chem.*, **45**, 553 (1973).

10) J. J. Kankare, *Anal. Chem.*, **42**, 1322 (1970).

11) M. Takatsuki and K. Yamaoka, *J. Sci. Hiroshima Univ. Ser. A*, **40**, 387 (1976).

12) K. Yamaoka and M. Takatsuki, *Bull. Chem. Soc. Jpn.*, **51**, 3182 (1978).

13) M. Takatsuki and K. Yamaoka, *Bull. Chem. Soc. Jpn.*, **52**, 1003 (1979).

14) N. Greenfield, B. Davidson, and G. D. Fasman, *Biochemistry*, **6**, 1630 (1967).

15) N. Greenfield and G. D. Fasman, *Biochemistry*, **8**, 4108 (1969).

16) Y. H. Chen, J. T. Yang, and H. M. Martinez, *Biochemistry*, **11**, 4120 (1972).

17) Y. H. Chen, J. T. Yang, and K. H. Chau, *Bicchemistry*, **13**, 3350 (1974).

18) C. C. Baker and I. Isenberg, *Biochemistry*, **15**, 629 (1976).

19) C. Djerassi, "Optical Rotatory Dispersion," McGraw-Hill Book Co., New York (1960), p. 160.

20) J. Y. Cassim and J. T. Yang, *Biopolymers*, **9**, 1475 (1970).

21) K. Yamaoka and T. Masujima, *Bull. Chem. Soc. Jpn.*, **52**, 1286 (1979).

22) A. Katchalsky and P. Spitnik, *J. Polymer Sci.*, **2**, 432 (1947).

23) H. P. Gregor and M. Frederick, *J. Polymer Sci.*, **23**, 451 (1957).

24) J. R. Parrish, Jr., and E. R. Blout, *Biopolymers*, **10**, 1491 (1971).